Surface-Enhanced Raman Scattering

DOI: 10.1002/anie.200804059

Au@pNIPAM Colloids as Molecular Traps for Surface-Enhanced, Spectroscopic, Ultra-Sensitive Analysis**

Ramon A. Álvarez-Puebla, Rafael Contreras-Cáceres, Isabel Pastoriza-Santos, Jorge Pérez-Juste, and Luis M. Liz-Marzán**

Surface-enhanced Raman scattering (SERS) is a powerful analytical technique that allows ultra-sensitive chemical or biochemical analysis.[1] Since the first reported SERS on silver and gold colloids in 1979,[2] they have become one of the most commonly used nanostructures for SERS, both as a testing ground for the most thorough theoretical modeling, and for the achievement of single-molecule detection (SMD).[3] Analytical applications based on average SERS are mature, and current work is focused on specific tuning of the experimental conditions for each particular analyte. For example, the enhancement factors (EF) reported for organic acids and alcohols are several orders of magnitude lower than those achieved for thiols and amines. The main reason for this situation is the different affinity of the functional groups in the analyte toward colloidal gold or silver surfaces, and it is the affinity which determines the analytes retention.[4] To circumvent this problem, various approaches have been proposed, including the functionalization of silver nanoparticles with different surface functional groups (e.g. calixarenes, viologen derivatives),[5] so as to increase their compatibility with polycyclic aromatic compounds. A problem inherent to this alternative is that usually the assembled molecules provide strong SERS signals that overlap and screen those corresponding to the analyte. Another alternative relies on controlling the surface charge of the nanoparticles to promote the electrostatic attraction of the analyte onto the particle surface.[6] This approach has been reported to consistently enhance the signal for acids and amines, but it hardly helps in the case of alcohols, ethers, and other oxygen-containing groups, as well as for non-functionalized molecules. Therefore, there is a clear need for development of colloidal systems containing a noble-metal component together with a material that can trap a wide variety of molecular analytes.

Herein we present the application of a recently developed core–shell colloidal material[7] comprising gold nanoparticles coated with a thermally responsive poly-(*N*-isopropylacrylamide) (pNIPAM) microgel, which we denote Au@pNIPAM. While the gold cores provide the necessary enhancing properties, the pNIPAM shells can swell or collapse as a function of temperature, this change is expected to serve as a means to trap molecules and get them sufficiently close to the metal core for providing the SERS signal. Although similar systems have been proposed for applications in catalysis,[8] temperature and pH sensing,[9] or light-responsive materials,[10] we propose that our particular configuration, with sufficiently big metal cores, can function as a general sensor for detection of all types of analytes. Apart from the SERS enhancement, this system can also be used to modulate the fluorescence intensity of adsorbed chromophores as a function of temperature. It is important to note that, the porous, protective pNIPAM shell not only enhances the long-term colloidal stability of the system in aqueous solutions, but additionally prevents electromagnetic coupling between metal particles, thus providing highly reproducible SERS signal and intensity, which is crucial for quantitative applications. Through a rational choice of model analytes, we demonstrate the application of these thermoresponsive hybrid materials for surface-enhanced Raman scattering, fluorescence, and resonance Raman scattering (SERS, SEF, and SERRS, respectively). This demonstration includes the first report of the SERS spectrum of 1-naphthol, which had remained elusive to SERS ultra-sensitive analysis until now. 1-Naphthol is a relevant biomarker for quantifying the exposure to polycyclic aromatic hydrocarbons in urine,[11] as well as the presence of carbaryl pesticides in the environment and in fruits.[12] Additionally, chronic exposure of humans to 1-naphthol has been reported to result in genotoxicity.[13]

The synthesis of the core–shell Au@pNIPAM colloids has been described in detail elsewhere[7] and involves initial growth of a thin polystyrene (PS) shell on cetyl trimethyl ammonium bromide (CTAB) coated, 67 nm gold nanoparticles, followed by polymerization of *N*-isopropylacrylamide (NIPAM) and a cross-linker (*N*,*N*-methylenebisacrylamide; see Experimental Section for details). NIPAM monomers are polymerized in situ on the Au@PS surfaces using 2,2′-azobis(2-methylpropionamidine) dihydrochloride (AAPH) as an initiator (Scheme 1a and Figure 1a). Particles with larger metal cores (116 nm) were prepared by seeded growth of the coated gold cores through addition of $HAuCl_4$ and ascorbic acid (Figure 1b). The SERS spectrum of Au@PS

[*] Dr. R. A. Álvarez-Puebla, Dr. I. Pastoriza-Santos, Dr. J. Pérez-Juste, Prof. L. M. Liz-Marzán
Departamento de Química-Física and Unidad Asociada CSIC-Universidade de Vigo, 36310 Vigo (Spain)
http://webs.uvigo.es/coloides/nano
E-mail: ramon.alvarez@uvigo.es
lmarzan@uvigo.es
R. Contreras-Cáceres
Departamento de Física Aplicada
Universidad de Almería, Almería (Spain)

[**] This work has been funded by the Spanish Ministerio de Ciencia e Innovación (MAT2007-62696 and MAT2008-05755/MAT), COST action D43, the Xunta de Galicia (PGIDIT06TMT31402PR), and Junta de Andalucia ("Excellence Project": FQM-02353).

Supporting information for this article is available on the WWW under http://dx.doi.org/10.1002/anie.200804059.

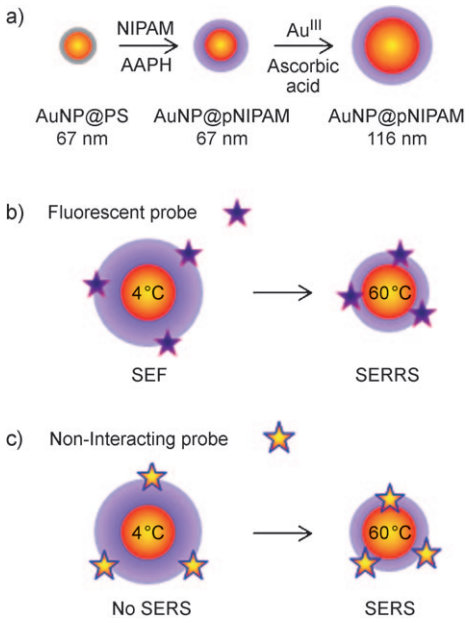

Scheme 1. Schematic representation of the fabrication (a), and the application of thermoresponsive Au@pNIPAM microgels for surface-enhanced fluorescence (SEF) and surface-enhanced resonance Raman scattering (SERRS) (b), and as molecular traps for surface-enhanced Raman scattering (SERS) of non-interacting molecular probes (c).

(Figure S1, Supporting Information), measured from a precipitated powder, shows the ring C=C stretching (1615 cm^{-1}), CH_2 scissoring (1461 cm^{-1}), ring breathing (1012 cm^{-1}), and radial ring stretching mode (646 cm^{-1}) bands, which are characteristic of polystyrene.[14] Notably, all these bands are no longer observed upon formation of the pNIPAM shell (Figure S1, Supporting Information), indicating either the replacement of PS by pNIPAM or the absence of hot spots as a result of the screening of plasmon coupling when the separation between Au particles is increased. The SERS spectra measured from Au@pNIPAM for both selected core sizes (67 and 116 nm), fit band to band, both being characterized by the NH bending (1447 cm^{-1}), CN stretching (1210 cm^{-1}), CH_3 rocking (963 cm^{-1}), CH deformation (866 and 841 cm^{-1}), CC rocking (766 cm^{-1}), CNO bending (655 cm^{-1}), and CCO out-of-plane deformation (413 cm^{-1}). The substantial differences in intensity are indicative of a considerable increase in optical enhancing properties of the larger gold cores, in agreement with previous reports.[15] Importantly, the overall SERS intensity (cross-section) obtained from pNIPAM is low, thus providing an excellent background for detection applications. Characterization of the localized surface plasmon resonances (LSPR, Figure 1c) for both samples show a notable red-shift when the particle size is increased, whereas the effect of temperature on the plasmonic response is modest. As we reported earlier, the LSPR bands red-shift upon collapse of the pNIPAM shell, owing to the associated local refractive index increase around the gold particles.[7,16]

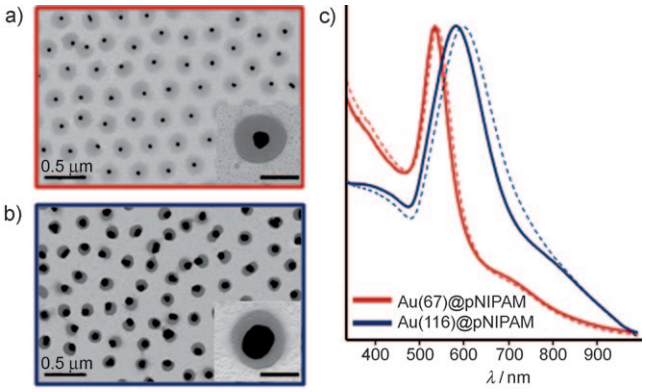

Figure 1. Representative TEM images of Au@pNIPAM core–shell particles, with Au cores of a) 67 nm and b) 116 nm diameter. Insets: magnifications of a single core–shell particle (scale bars: 100 nm). c) UV/Vis spectra of aqueous suspensions of both Au@pNIPAM microgel colloids, measured at 4 °C (solid lines) and 60 °C (broken lines).

The optical enhancing properties of the Au@pNIPAM colloids were initially tested using 1-naphthalenethiol (1NAT) as a model analyte, because it is a small molecule with a large affinity for gold (through the thiol group), which should easily diffuse through the porous polymer shell, and its SERS spectrum is well established.[17] The SERS spectrum of 1NAT (Figure 2a) is dominated by the ring stretching (1553, 1503, and 1368 cm^{-1}), CH bending (1197 cm^{-1}), ring breathing (968 and 822 cm^{-1}), ring deformation (792, 664, 539, and 517 cm^{-1}), and CS stretching (389 cm^{-1}). The most interesting property of pNIPAM microgels is a phase transition from a hydrophilic, water-swollen state into a hydrophobic, globular state when heated above their lower critical solution temperature (LCST) which is about 32 °C, in water. Gel compression is related to dehydration, and gives rise to final collapsed volumes of less than 50 % the swollen microgel volume,[18] this transition is completely reversible.[7] Thus, when 1NAT is added to the swollen Au@pNIPAM colloid (Figure 2b), the analyte can easily diffuse through the polymer network until reaching the gold-core surface, to which it readily chemisorbs. This is reflected in the high SERS intensity recorded at 4 °C, which remains high after gradually heating up to 60 °C and

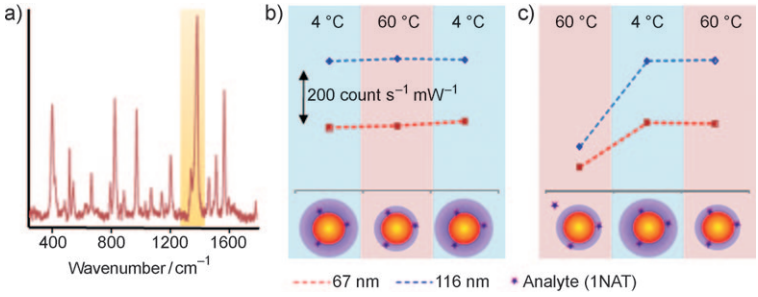

Figure 2. a) SERS spectrum of 1-napthalenethiol (λ_{ex} = 785 nm) in Au@pNIPAM aqueous dispersions. Variation of the intensity of the band at 1368 cm^{-1} (ring stretching; highlighted in yellow), as a function of gold-core size and solution temperature in two different cooling-heating cycles: b) from 4 to 60 to 4 °C; and, c) from 60 to 4 to 60 °C. The intensity scale is common for (b) and (c). Acquisition time was 2 s in all cases.

cooling down back to 4 °C. However, when 1NAT is added to a dispersion of the collapsed microgel (60 °C), the measured SERS signal is substantially lower (Figure 2c). Cooling this suspension down to 4 °C leads to an increase of the signal to an intensity that is comparable to that of the previous cycle. The signal remains stable during subsequent temperature changes. From these results we can conclude that, when the gel is swollen, 1NAT can indeed diffuse freely through the network, but when the microgel is collapsed, diffusion of the analyte is hindered and the gold surface cannot be reached. However, once 1NAT has been adsorbed, it stays retained regardless of the swollen or collapsed state of the microgel. This result is consistent with the formation of a covalent Au–S bond, which has been often reported and is additionally confirmed by the disappearance of the SH stretching peak in the SERS spectra (Figure S2, Supporting Information).[17] It is interesting to note that precisely the same trend was observed for core–shell colloids with different particle sizes, but the enhancement provided by the larger, 116 nm Au cores is considerable higher than that from the 67 nm particles, partly because of the better match of the excitation wavelength (785 nm) with the plasmon band (see Figure 1).[15] Therefore, in all the experiments described below for the design of other analytical applications of these materials, only the Au@pNIPAM particles with 116 nm Au cores were employed. A final, interesting observation from this first experiment is the calculation of an enhancement factor (EF) of 5.16×10^5 (see Experimental Section and Supporting Information for details on EF calculation). Since pure 1NAT (as all aromatic thiols) does not present substantial charge-transfer-related enhancement (the so-called chemical effect),[19] the calculated EF is rather high, in particular considering that the microgel shell surrounding the Au particles prevents electromagnetic coupling, and consequently the formation of hot spots.

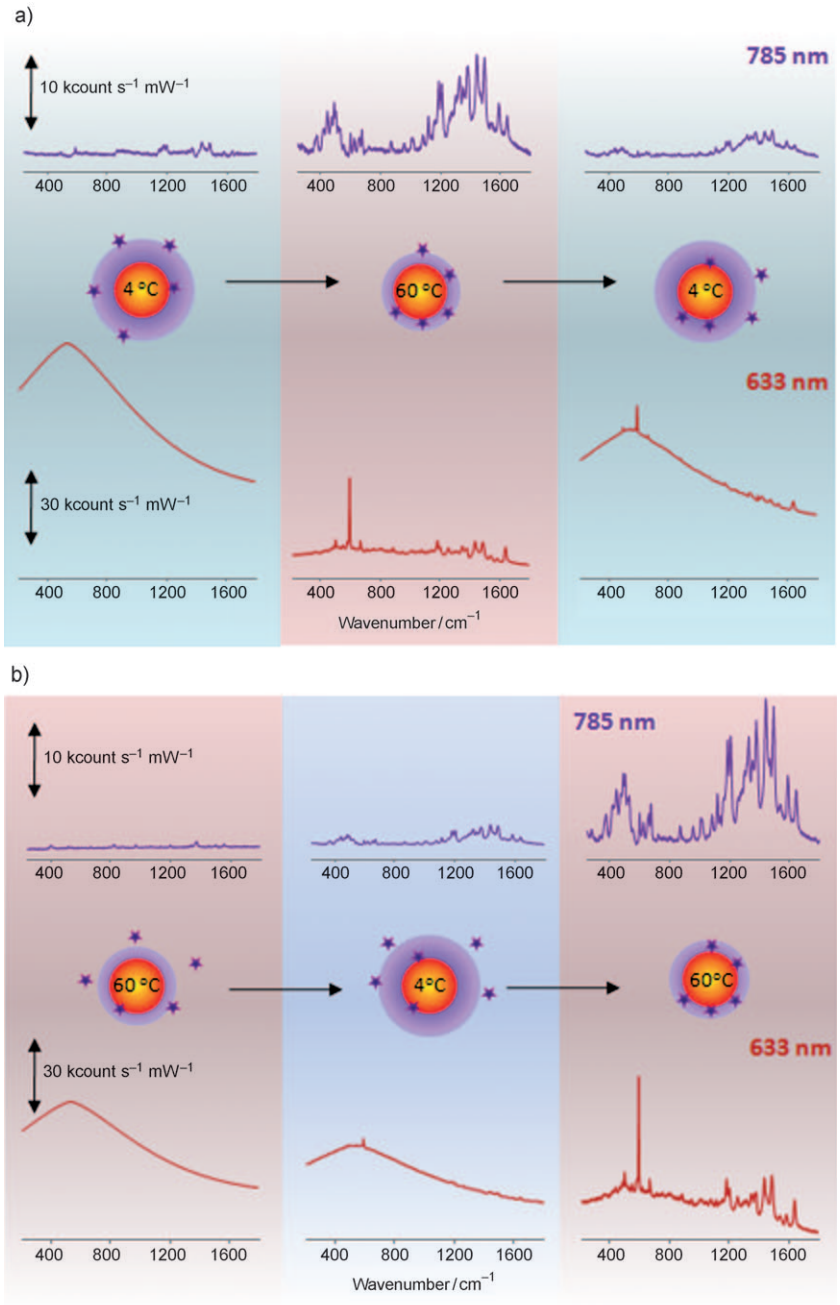

Figure 3. Variation of the SERS ($\lambda_{ex} = 785$ nm; blue trace) and SEF/SERRS ($\lambda_{ex} = 633$ nm; red trace) intensity of Nile Blue A, as a function of solution temperature in two different cooling–heating cycles: a) from 4 to 60 to 4 °C; and, b) from 60 to 4 to 60 °C. The intensity scale is common for (a) and (b). Acquisition time 2 s.

A second demonstration of the trapping properties of the Au@pNIPAM system (Scheme 1b) is provided in Figure 3, which shows results for the heating–cooling cycles, using a common dye, Nile Blue A (NBA) as a molecular probe. The NBA molecule is slightly larger than 1NAT and, in addition, it contains an amine functional group, so that its affinity for gold is lower than that of 1NAT.[4] Another interesting property of NBA is that it gives different spectra (either SERS or SEF/SERRS) depending on the excitation wavelength. Upon excitation with a near-IR (NIR, 785 nm) laser line, far away from the electronic absorption band (Figure S3, Supporting Information), NBA supported onto an optical enhancer will produce a normal SERS signal. On the contrary, if NBA is excited with a red laser (633 nm) perfectly matching its absorption band (Figure S3, Supporting Information) either SERRS or SEF will be produced, depending on the distance to the metal nanostructure. If the molecule is close enough to the metal, the fluorescence will be quenched, whereas if the molecule is close but not next to the metal, it will feel the

electromagnetic field enhancement generated by the nanostructure. Though SERRS and SERS spectra fit band to band, the relative intensities are different because in SERRS not only the surface selection rules[20] but also the resonance effects[21] are to be considered. Briefly, both the SERS and SERRS spectra are characterized by ring stretching (1643, 1492, 1440, 1387, 1351, and 1325 cm^{-1}), CH bending (1258, 1185 cm^{-1}), and the in-plane CCC and NCC (673 cm^{-1}), CCC and CNC (595 cm^{-1}), and CCC (499 cm^{-1}) deformations.[22] The bands at 673 and 595 cm^{-1} are significantly more enhanced in SERRS than in SERS, indicating that they correspond to the chromophore (in this case the phenoxazine) and the electronic resonance tends to enhance scattering bands from chemical groups that absorb the excitation laser line. On the other hand, enhanced fluorescence (SEF)[23] spectra are very similar to those for standard fluorescence, with a maximum emission at 668 nm.

When NBA was added to the swollen colloid (4 °C, Figure 3 a), and excited with the NIR laser line, the recorded SERS intensity was very weak. However, the intensity notably increased with temperature and gel collapse, decreasing again after cooling. When the same samples were excited with the red line, the spectrum of the initial, swollen sample showed intense fluorescence, which can be readily described as SEF, as the intensity was 16-fold that of normal fluorescence. However, when the temperature was increased to 60 °C (gel collapse), the fluorescence was completely quenched, and the SERRS spectrum was obtained. After subsequent cooling to 4 °C, a less-intense SERRS spectrum could still be identified on top of a strong SEF background. Because of the difference in the affinity of amines and thiols for gold, the retention of NBA is not as stable as that of 1NAT, as reflected in the decrease in SERS and SERRS, along with the increase in SEF, when the sample was swollen again, indicating partial release of NBA molecules. Interestingly, when the inverse cycle (60–4–60 °C, Figure 3 b) was applied, strong SEF intensity was recorded at 60 °C, which turned upon gel expansion into a weak SERRS signal (4 °C), with complete fluorescence quenching, and then to an intense SERRS signal after final heating, back to 60 °C. Interpretation of these results is as follows. Swollen pNIPAM does not allow the adsorption of NBA onto the gold cores (as indicated by a very weak SERS signal at 4 °C), but it does trap the analyte molecules within the polymer gel network (strong SEF completely screening the SERRS signal). When the temperature is raised up to 60 °C, the shell is collapsed and NBA molecules are trapped closer to the cores, as indicated by notable increases of SERS and SERRS, while SEF is quenched. Temperature sensitivity of fluorescence enhancement has been reported by Kotov and co-workers for Au nanoparticles linked to quantum dots through a thermoresponsive molecule.[24] In the second cycle (60–4–60 °C), a similar behavior was observed. For the original, collapsed microgel, only SEF is recorded, but upon swelling and subsequent collapse, NBA is retained in close contact with the gold core surface. This trapping effect is very likely related to the hydrophilic–hydrophobic transition, as well as dehydration and microcapillarity effects during microgel collapse.[18] Thus, these Au@pNIPAM microgels can provide a fine control on the nature of the measured signal by simply controlling the solution temperature.

Finally, and probably most remarkably, the described trapping effect can be applied to the SERS identification of molecules such as 1-napthol, which had not been possible to date because it does not easily adsorb onto conventional silver or gold surfaces (Scheme 1 c). Thus, the 1-napthol SERS spectrum could be recorded for the first time (Figure 4), and found to be characterized by CH bending (1447 cm^{-1}), ring stretching (1390 cm^{-1}), CCC in-plane deformation (842 cm^{-1}), CH out-of-plane deformation, ring breathing (716 cm^{-1}), ring deformation (655 and 584 cm^{-1}) and, ring twisting (477 cm^{-1}), in close agreement with the Raman assignment reported by Lakshminarayan and Knee.[25] As shown in Figure 4, the SERS signal can only be properly identified after a swell–collapse transition, so that 1-napthol can first be retained within the polymer networks and then

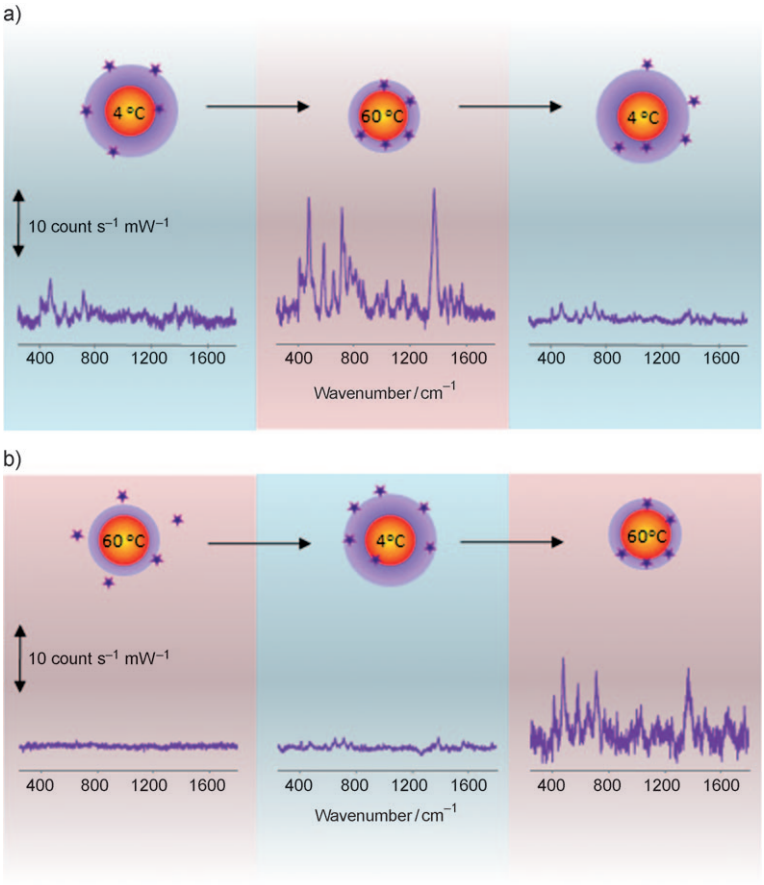

Figure 4. Variation of the SERS ($\lambda_{ex} = 785$ nm) intensity of 1-naphthol as a function of the solution temperature in two different cooling-heating cycles: b) from 4 to 60 to 4 °C; and, b) from 60 to 4 to 60 °C. The intensity scale is common for (a) and (b). Acquisition time 2 s.

brought into contact with the gold surface. Upon subsequent cooling, the microgel shell swells again and the 1-napthol molecules are totally released from the gold surface, resulting in a dramatic loss of SERS signal (Figure 4a). The low affinity of hydroxy groups for Au surfaces is very clearly reflected in the reversibility of the SERS signal along the swell–collapse cycles.

In summary, we have designed, characterized, and applied an advanced optical platform that allows for general, ultrasensitive analysis of a wide variety of molecules through surface enhanced spectroscopy. The unique thermoresponsive properties, high EF with no electromagnetic coupling, and the colloidal stability of these materials should find application in quantitative analysis through direct SERS/SERRS sensing,[26] fabrication of encoded particles[27] by using thiolated dyes,[28] or as solution fluorescence enhancers[29] for a variety of biomedical applications,[30] such as cellular uptake,[31] imaging,[32] or flow-citometry.[33]

Experimental Section

Gold nanoparticles encapsulated in thermoresponsive pNIPAM microgels were prepared as described elsewhere.[7] Briefly, AuNPs (average diameter (67 ± 5) nm) were prepared through a seeded growth method[34] by reduction of $HAuCl_4$ with ascorbic acid on CTAB-stabilized Au seeds (ca. 15 nm), in the presence of 0.015 M CTAB. Initial polystyrene coating of AuNPs was carried out as follows: as-prepared CTAB-stabilized AuNPs (150 mL) were centrifuged, the supernatant solution discarded, and the precipitate redispersed in milli-Q water (150 mL). The solution was then heated to 30 °C, followed by addition of styrene (10 μL) and divinylbenzene (5 μL) under stirring. After 15 min the temperature was further raised to 70 °C and polymerization was initiated by adding 2,2′-azobis(2-methylpropionamidine) dihydrochloride (AAPH, 20 μL, 0.1 M in water), and allowed to proceed for 2 h. The colloid was then washed by centrifugation and redispersion in milli-Q water (15 mL). The pNIPAM shell was grown by addition of *N*-isopropylacrylamide (NIPAM, 0.1698 g) and *N*,*N*-methylenebisacrylamide (0.0234 g) under nitrogen. After 15 min, the nitrogen flow was removed and the polymerization was initiated by adding AAPH (150 μL 0.1 M). The reaction was allowed to proceed for 3 h at 70 °C. The reddish-white mixture was then allowed to cool to room temperature under stirring. To remove small oligomers, residual monomers as well as gold-free microgels, the dispersion was diluted with water (15 mL), centrifuged, and redispersed in water three times.

Further in situ growth of the AuNP cores up to (116 ± 11) nm diameter was performed by adding CTAB (4.06 mL; 0.1 M) containing $HAuCl_4$ (0.125 mM) and ascorbic acid (0.25 mM) onto Au@pNIPAM (0.94 mL).

UV/Vis spectra were recorded using an Agilent 8453 UV/Vis diode array spectrophotometer. Transmission electron microscopy was carried out by using a JEOL JEM 1010 microscope operating at an acceleration voltage of 100 kV.

Raman, SERS, SERRS, and SEF were measured on a LabRam HR (Horiba-Jobin Yvon) Raman system. Microgel characterization was performed under the microscope by centrifuging 1 mL of the corresponding suspension and casting the residue on a glass slide, SERS was recorded by exciting the sample with a 785 nm laser line. SERS, SERRS and/or SEF of either, 1-naphtalenethiol (1NAT, Acros Organics), Nile Blue A (NBA, Aldrich) or 1-naphthol (1NOH, Aldrich) were recorded in suspension by using a macrosampling accessory. Two different experiments were designed. First, 1 mL aliquots of AuNP@pNIPAM (5×10^{-4} M in gold) were stabilized at 4 °C. Then, 10 μL of analyte was added to each NP suspension reaching final concentrations of 10^{-5} M for 1NAT and 1NOH and 10^{-6} M for NBA. After 2 h at 4 °C, time enough to reach thermodynamic equilibrium, the samples were excited with a 785 nm laser line to collect the SERS spectra. In the case of NBA, fluorescence emission and SERRS were excited by illuminating the sample with a 633 nm laser. Thereafter, the samples were equilibrated at 60 °C for 2 h and again at 4 °C. After each equilibration step, spectra were collected under the same conditions. In the second experiment, equilibration steps were repeated, but starting at 60 °C, cooling down to 4 °C and heating back to 60 °C. Again, spectra were collected after each step under identical conditions.

Approximate enhancement factors (EF) of AuNP@pNIPAM for SERS and SEF were estimated by applying Equation (1):[35]

$$EF = (I_A V_A / I_B V_B) f \quad (1)$$

Where V_A and V_B represent the probed volumes, and I_A and I_B the intensities in SERS and Raman, respectively; f, is a correction factor that considers the concentration ratio of the probed molecule in both experiments under the same conditions. Since 1NAT is a liquid, Raman spectra were collected directly, with no need for dissolution in any solvent. The concentration of pure 1NAT (7.18 M) was determined through its density ($\rho_{1NAT} = 1.15\ kg\,L^{-1}$). In the case of NBA, which is a solid, fluorescence was collected from a 10^{-5} M solution. Provided that V_A and V_B are similar, Equation (1) can be reduced to $EF = (I_A/I_B)f$, were f is 7.18×10^5 for 1NAT and 10 for NBA.

Received: August 16, 2008
Published online: November 27, 2008

Keywords: colloids · gold · nanoparticles · sensing · SERS

[1] K. Kneipp, H. Kneipp, I. Itzkan, R. R. Dasari, M. S. Feld, *Chem. Rev.* **1999**, *99*, 2957–2976.
[2] J. A. Creighton, C. G. Blatchford, M. G. Albretch, *J. Chem. Soc. Faraday Trans. 2* **1979**, *75*, 790–798.
[3] a) K. Kneipp, Y. Wang, H. Kneip, L. T. Perelman, I. Itzkan, R. R. Dasari, M. Feld, *Phys. Rev. Lett.* **1997**, *78*, 1667–1670; b) S. Nie, S. R. Emory, *Science* **1997**, *275*, 1102–1106.
[4] R. G. Pearson, *J. Am. Chem. Soc.* **1963**, *85*, 3533–3539; R. G. Pearson, *Science* **1966**, *151*, 172–177.
[5] a) L. Guerrini, J. V. Garcia-Ramos, C. Domingo, S. Sanchez-Cortes, *Langmuir* **2006**, *22*, 10924–10926; b) L. Guerrini, J. V. Garcia-Ramos, C. Domingo, S. Sanchez-Cortes, *J. Phys. Chem. C* **2008**, *112*, 7527–7530.
[6] a) R. A. Alvarez-Puebla, E. Arceo, P. J. G. Goulet, J. J. Garrido, R. F. Aroca, *J. Phys. Chem. B* **2005**, *109*, 3787–3792; b) R. F. Aroca, R. A. Alvarez-Puebla, N. Pieczonka, S. Sanchez-Cortes, J. V. Garcia-Ramos, *Adv. Colloid Interface Sci.* **2005**, *116*, 45–61.
[7] R. Contreras-Cáceres, A. Sánchez-Iglesias, M. Karg, I. Pastoriza-Santos, J. Pérez-Juste, J. Pacifico, T. Hellweg, A. Fernández-Barbero, L. M. Liz-Marzán, *Adv. Mater.* **2008**, *20*, 1666–1670.
[8] Y. Lu, Y. Mei, M. Drechsler, M. Ballauff, *Angew. Chem.* **2006**, *118*, 827–830; *Angew. Chem. Int. Ed.* **2006**, *45*, 813–816.
[9] J. H. Kim, T. R. Lee, *Chem. Mater.* **2004**, *16*, 3647–3651.
[10] I. Gorelikov, L. M. Field, E. Kumacheva, *J. Am. Chem. Soc.* **2004**, *126*, 15938–15939.
[11] a) A. M. Hansen, O. Omland, O. M. Poulsen, D. Sherson, T. Sigsgaard, J. M. Christensen, E. Overgaard, *Int. Arch. Occup. Environ. Health* **1994**, *65*, 385–394; b) M. Jakubowski, M. Trzcinka-Ochocka, *J. Occup. Health* **2005**, *47*, 22–28.
[12] H. Sun, O.-X. Shen, X.-L. Xu, L. Song, X.-R. Wang, *Toxicology* **2008**, *249*, 238–242.
[13] a) W. J. Kozumbo, S. Agarwal, H. S. Koren, *Toxicol. Appl. Pharmacol.* **1992**, *115*, 107–115; b) K. Grancharov, H. Engel-

berg, Z. Naydenova, G. Müller, A. W. Rettenmeier, E. Golovinsky, *Arch. Toxicol.* **2001**, *75*, 609 – 612.
[14] P. P. Hong, F. J. Boerio, S. D. Smith, *Macromolecules* **1993**, *26*, 1460 – 1464.
[15] a) K. L. Kelly, E. Coronado, L. L. Zhao, G. C. Schatz, *J. Phys. Chem. B* **2003**, *107*, 668 – 677; b) P. N. Njoki, I.-I. S. Lim, D. Mott, H.-Y. Park, B. Khan, S. Mishra, R. Sujakumar, J. Luo, C.-J. Zhong, *J. Phys. Chem. C* **2007**, *111*, 14664 – 14669.
[16] M. Karg, I. Pastoriza-Santos, J. Pérez-Juste, T. Hellweg, L. M. Liz-Marzán, *Small* **2007**, *3*, 1222 – 1229.
[17] R. A. Alvarez-Puebla, D. S. Dos Santos, Jr, R. F. Aroca, *Analyst* **2004**, *129*, 1251 – 1256.
[18] B. Sierra-Martin, Y. Choi, M. S. Romero-Cano, T. Cosgrove, B. Vincent, A. Fernandez-Barbero, *Macromolecules* **2005**, *38*, 10782 – 10787.
[19] A. D. McFarland, M. A. Young, J. A. Dieringer, R. P. Van Duyne, *J. Phys. Chem. B* **2005**, *109*, 11279 – 11285.
[20] a) M. Moskovits, J. S. Suh, *J. Phys. Chem.* **1984**, *88*, 5526 – 5530; b) M. Moskovits, *Rev. Mod. Phys.* **1985**, *57*, 783 – 826.
[21] D. A. Long, *The Raman Effect: A Unified Treatment of the Theory of Raman Scattering by Molecules*, Wiley, Chichester, **2002**.
[22] S. Millera, N. D. A. Aiker, *J. Chem. Soc. Faraday Trans. 1* **1984**, *80*, 1305 – 1312.
[23] K. Aslan, J. R. Lakowicz, C. D. Geddes, *Anal. Bioanal. Chem.* **2005**, *382*, 926 – 933.
[24] J. Lee, A. O. Govorov, N. A. Kotov, *Angew. Chem.* **2005**, *117*, 7605 – 7608; *Angew. Chem. Int. Ed.* **2005**, *44*, 7439 – 7442.
[25] C. Lakshminarayan, J. L. Knee, *J. Phys. Chem.* **1990**, *94*, 2637 – 2643.
[26] S. E. J. Bell, N. M. S. Sirimuthu, *Chem. Soc. Rev.* **2008**, *37*, 1012 – 1024.
[27] K. Braeckmans, S. C. De Smedt, M. Leblans, C. Roelant, J. Demeester, *Nat. Rev. Drug Discovery* **2002**, *1*, 1 – 10.
[28] L. O. Brown, S. K. Doorn, *Langmuir* **2008**, *24*, 2178 – 2185.
[29] K. Aslan, M. Wu, J. R. Lakowicz, C. D. Geddes, *J. Am. Chem. Soc.* **2007**, *129*, 1524 – 1525.
[30] S. G. Penn, L. He, M. J. Natan, *Curr. Opin. Chem. Biol.* **2003**, *7*, 609 – 615.
[31] J. Kneipp, H. Kneipp, M. McLaughlin, D. Brown, K. Kneipp, *Nano Lett.* **2006**, *6*, 2225 – 2231.
[32] X.-M. Qian, S. M. Nie, *Chem. Soc. Rev.* **2008**, *37*, 912 – 920.
[33] D. A. Watson, L. O. Brown, D. F. Gaskill, M. Naivar, S. W. Graves, S. K. Doorn, J. P. Nolan, *Cytometry Part A* **2008**, *73*, 119 – 128.
[34] J. Rodriguez-Fernandez, J. Perez-Juste, F. J. Garcia de Abajo, L. M. Liz-Marzan, *Langmuir* **2006**, *22*, 7007 – 7010.
[35] R. Alvarez-Puebla, D. S. Santos, R. F. Aroca, *Analyst* **2007**, *132*, 1210 – 1214.

